

Dynamics of a Deformable Body in a Fast Flowing Soap Film

Sunghwan Jung,¹ Kathleen Mareck,¹ Michael Shelley,¹ and Jun Zhang^{2,1}

¹*Applied Mathematics Laboratory, Courant Institute of Mathematical Sciences, New York University, 251 Mercer Street, New York, New York 10012, USA*

²*Department of Physics, New York University, 4 Washington Place, New York, New York 10003, USA*

(Received 29 May 2006; published 28 September 2006)

We study the behavior of an elastic loop embedded in a flowing soap film. This deformable loop is wetted into the film and is held fixed at a single point against the oncoming flow. We interpret this system as a two-dimensional flexible body interacting in a two-dimensional flow. This coupled fluid-structure system shows bistability, with both stationary and oscillatory states. In its stationary state, the loop remains essentially motionless and its wake is a von Kármán vortex street. In its oscillatory state, the loop sheds two vortex dipoles, or more complicated vortical structures, within each oscillation period. We find that the oscillation frequency of the loop is linearly proportional to the flow velocity, and that the measured Strouhal numbers can be separated based on wake structure.

DOI: [10.1103/PhysRevLett.97.134502](https://doi.org/10.1103/PhysRevLett.97.134502)

PACS numbers: 47.32.ck, 47.20.-k, 47.54.De

The wake flow behind a rigid obstacle is a central object of study in fluid mechanics. When the oncoming flow velocity exceeds a threshold, vortices are shed behind the obstacle [1]. A typical wake is composed of successive eddies of alternating sign—the “von Kármán vortex street”—and is observed over a wide range of flow velocities and body shapes [2,3]. The frequency of vortex shedding (f) is determined by the flow velocity (V) and the object size (d), whose relation is captured by the near constancy of the Strouhal number, $St = df/V$ [3].

The dynamics of a rigid object which moves freely in the direction perpendicular to the flow is of interest in many industrial and biological applications [4–8]. Lateral motion of an object can be induced by interaction with the flow and is often called *vortex-induced vibration* (VIV). At low flow velocities, the body starts to oscillate sideways with a small amplitude (less than 0.4 times body diameter). Its associated wake structure is again a von Kármán vortex street. However, further increase of flow velocity causes the obstacle to oscillate in phase with the vortex shedding, and as a result, a series of dipoles are shed [7,8].

Settling bodies or rising bubbles, where the balance of gravitational and drag forces set the velocity, also exhibit transitions as they interact with their wakes. For example, a slowly settling sedimenting sphere falls straight downwards [9] but above a certain sedimentation velocity, the sphere’s motion becomes periodic and its trajectory a spiral or zigzag [10]. A *deformable* object, such as a droplet or bubble, can behave similarly even as its shape now changes [11,12].

Finally, studies have shown the instability (and bistability) of slender deformable bodies to lateral oscillations in quasi-2D soap film flows [13], and of heavy deformable sheets to lateral oscillations in fast 3D flows [14–17]. In these cases, the system corresponds to the flapping of a flag in a stiff breeze.

Flowing soap film provides a practical template upon which to study the dynamics of a nearly 2D flow [18,19]. The experimental setup has been introduced earlier [13,18–20]. In this work, we introduce a deformable closed body into a fast soap film flow. Two thin nylon wires (0.3 mm in diameter) separate at a nozzle (0.5 mm inner diameter) attached to the bottom of a reservoir. The reservoir contains soapy water maintained at a fixed pressure head, thus fixing the flux. A stopcock regulates the flow rate through the nozzle. The nylon wires extend downwards to a collection box 2.4 m below. Driven by gravity, the soap film flows downwards. Owing to air drag, a terminal velocity is reached approximately 60 cm below the nozzle with a velocity profile near the center close to being uniform (velocity differences are within 20% of the mean, over 60% of the span about the midline). From optical interference patterns, the film thickness is found to vary smoothly across the film by about 15% of its average thickness.

We use a thin rubber loop (0.2 mm thick) as the deformable structure. The loop wets into the soap film and is supported from its inner side against the flow. The loop is much thicker than the soap film ($\sim 3 \mu\text{m}$) and we do not typically observe leakage across the loop. Six loops of different circumferences (5–7.5 cm) are used. We find that for regimes studied here, the loop appears to undergo only bending deformations, and not stretching or compression, as its length shows no measurable increase or decrease. Currently, we do not understand what balance of effects sets the enclosed area of the loop, which is an important constraint on the possible dynamics. However, we do find that, once experimental conditions are fixed, and the loop is in a fixed state of dynamics, the enclosed area changes very little in time (e.g. $\sim 5\%$ for a 5 cm loop). However, between different states or conditions, the enclosed area can vary by factors of two or three.

A laser Doppler velocimeter (LDV; Model LDP-100, TSI Inc.) is used to record the upstream velocity V . Micron-sized particles (TiO_2) are seeded into the flow for LDV measurements. Flow structures are visualized using interference patterns from monochromatic illumination (low-pressure sodium lamps operating at wavelength 585 nm). The movies of the wake flow together with the loop are recorded using a high-speed camera at 1000 frames per second.

The interaction between the loop and the flow is quite complicated. In our experiments, we observe bistable states, one stationary and another oscillatory [see Fig. 1(a) and 1(b)], that coexist over a range of flow velocities. At least in the conditions considered here, we do not observe spontaneous transitions between these two states. However, a transition from the stationary to the oscillatory state can be induced by externally perturbing the loop, or by abruptly changing the flow velocity.

In the stationary state, the loop behaves as a rigid hoop and has a teardrop shape with higher curvature on the top than on the sides [Fig. 1(a)]. A characteristic length scale (D) of the loop, its width in the film, is 1 cm. The flow

velocity (V) varies from 1.5 to 2.5 m/s and the kinematic viscosity (ν) of soap film is approximately $0.04 \text{ cm}^2/\text{s}$. The frequency of vortex shedding (f_s) varies from 20 to 50 Hz. Based on these characteristic numbers, we estimate the Reynolds number (Re) and Strouhal number (St_s) for the system to be

$$\text{Re} = \frac{VD}{\nu} \sim 5000, \quad \text{St}_s = \frac{Df_s}{V} \sim 0.2, \quad (1)$$

where the subscript s stands for vortex shedding, since the Strouhal number is calculated based on the vortical structure of the wake. Figure 1(a) shows the deforming body and its vortical wake using a 5 cm loop and flow velocity of 2.2 m/s. As can be seen, vortices of alternating sign are successively produced.

In the coexisting oscillatory state, shown in Fig. 1(b) at the same parameters as above, the loop now oscillates periodically in the horizontal direction, and the vortical wake behind it is quite different. For low flow velocity, two dipole pairs are shed during each oscillation period. Such a wake structure is also observed behind oscillating cylinders and is referred to as the $2P$ mode [8,21]. For both of these states, unsteady time-dependent wakes are shed behind the loop. This bistability is different from that observed at the onset of time-dependent vortex shedding from a cylinder fixed in a soap film flow [22].

Figure 2(a) shows both the position of the loop at several time points during one period of oscillation, and the path taken by its centroid. During the oscillation, the loop continuously changes its shape, and its centroid moves along a figure-eight trajectory [Fig. 2(a)]. This figure-eight shape is due to the fact that the frequency of oscillation in



FIG. 1. Flow structures behind a 5 cm loop at 2.2 m/s flow velocity. The coupled fluid-structure system shows bistability: (a) the stationary state; the loop remains essentially motionless and its wake is a von Kármán vortex street. The loop is deformed by the flow into a teardrop shape. (b) The oscillatory state; the loop sheds two vortex dipoles within each oscillation period.

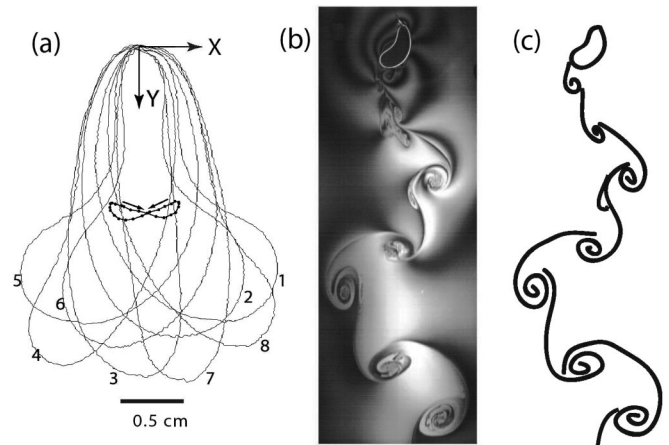


FIG. 2. (a) At 2.2 m/s flow velocity, eight snapshots of a 5 cm loop and its centroid are shown. The oscillation period of the oscillating loop is 52 ms. The snapshots of the flexible loop are presented as solid loops at 6 ms intervals and the trajectory of the centroid of the loop with 2 ms intervals. The loops are sequentially numbered. (b) Wake structure when the loop centroid is at the far left. The loop starts to shed a counter-clockwise vortex. The wake structure is schematically shown in (c).

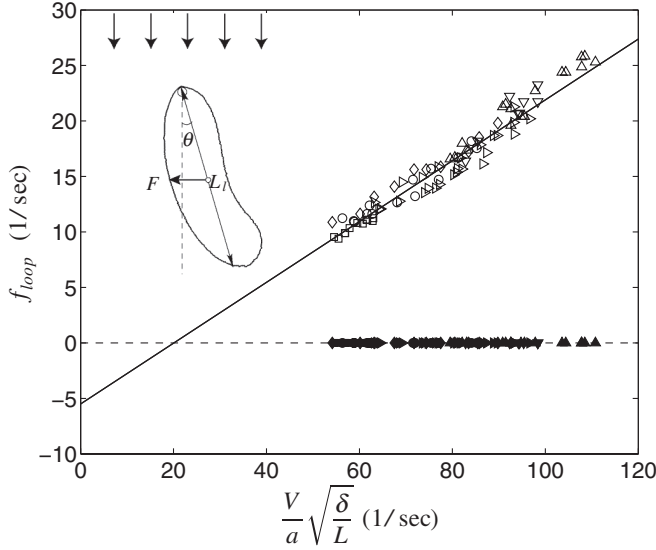


FIG. 3. Frequency of an oscillating loop (f_{loop}) versus rescaled velocity ($V\sqrt{\delta}/a\sqrt{L}$). We test over 6 different loop lengths [5 cm (Δ), 5.5 cm (∇), 6 cm (\triangleright), 6.5 cm (\diamond), 7 cm (\square), and 7.5 cm (\circ)]. The open symbols are in the oscillatory state and the closed ones are in the stationary state. The frequency of the oscillating loop is linearly proportional to the rescaled velocity.

the streamwise direction is twice that in the transverse direction. This has been observed in the motions of a flapping flag [13] and VIV systems [5,23]. Also, the loop oscillates in phase with that vortex shedding [Fig. 2(b) and 2(c)]. When the loop is at far right (or left), a clockwise turning (or counter-clockwise) vortex is shed.

By using loops of several different lengths, we find a linear relation between the oscillation frequency of the loop (f_{loop}) and a rescaled velocity $V\sqrt{\delta}/a\sqrt{L}$ (see Fig. 3), where δ is the film thickness, a the thickness of the loop, and L the loop length. Our results from loops of different lengths and differing flow velocities all collapse onto a single line with slope of about 0.27. The offset of this affine relation suggests a bifurcation to oscillation at a finite flow velocity; linear extrapolation to $f_{loop} = 0$ suggests a critical rescaled velocity of about 20, which is unfortunately below the reach of this experiment.

To better understand the relation between oscillation frequency and flow velocity, we propose a simple model for the oscillations of an elongated loop with longitudinal length L_i driven by a “lift force” in the direction perpendicular to the stream. The lift force (F) is taken as proportional to $\rho V^2 L_i \delta$, where ρ is the density of fluid, V the fluid velocity. Hence, $F = (1/2)C_L \rho V^2 L_i \delta$, where C_L is a lift coefficient. Typically, L_i is proportional to the loop circumference, L . At an angle θ inclined to the flow stream, C_L is proportional to $\sin\theta$ [24]. For small θ , $\sin\theta \sim x_{cm}/y_{cm}$ where x_{cm} , y_{cm} is the center of mass (centroid) location. Therefore, we approximate the lift force as $F = m\ddot{x}_{cm} \approx (1/2)\rho V^2 L_i \delta x_{cm}/y_{cm}$, where \ddot{x}_{cm} is the acceleration in the transverse direction and m is the total body

mass. In this experiment, the mass of the (wetted) loop is much greater than that of the enclosed fluid. Hence, we assume that the total body mass (m) is proportional to $\rho_L L a^2$ where ρ_L is the density of the loop. Also, the y component of the centroid, y_{cm} , and the length L_i are assumed to be proportional to the length of the loop if the body is elongated due to the flow. With the trivial solution for the x component of centroid, $x_{cm} = Ce^{i\omega t}$, we obtain an expression for the oscillation frequency: $\omega = 2\pi f_{loop} \propto V\sqrt{\delta}/a\sqrt{L}$. This is consistent with our observations and underlies our rescaling of the data in Fig. 3. Put differently, this is simply the oscillation frequency of a hanging pendulum where the gravitational force is replaced by a drag force.

As the flow velocity increases, a more complicated mode in the oscillatory state can be observed (left panel in Fig. 4). In this case, the loop sheds more than four vortices over a single period of oscillation. We refer to this wake structure as a *flaglike mode*. We use this terminology because the wake now resembles more that behind a flapping flag (see [13]), and because the body itself looks elongated and “flaglike”. This is because the enclosed area is now smaller in relation to L^2 than for the body in the $2P$ mode. To characterize the loop oscillation and the wake structure, we again define a Strouhal number, now using the oscillation frequency of the loop itself, or $St_L = Af_{loop}/V$ where A is the outer amplitude of oscillation as indicated in Fig. 4. The corresponding Strouhal numbers

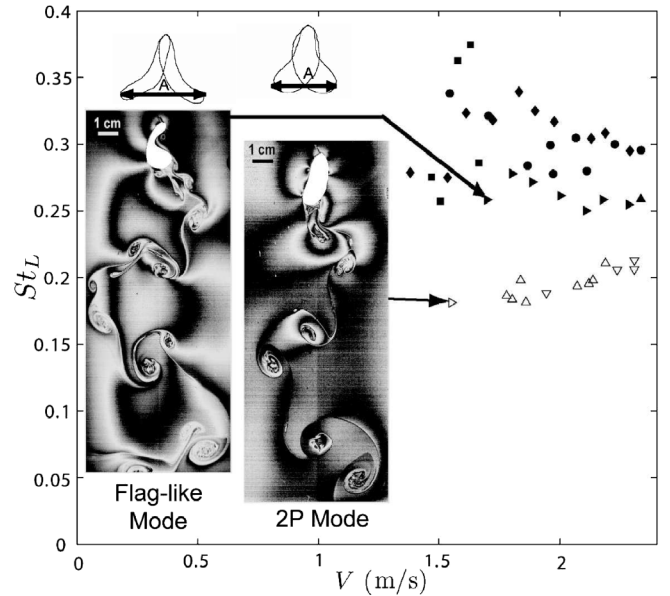


FIG. 4. Strouhal number of the loop (St_L) versus the flow velocity (V) for different loop lengths [5 cm (Δ), 5.5 cm (∇), 6 cm (\triangleright), 6.5 cm (\diamond), 7 cm (\square), and 7.5 cm (\circ)]. Open symbols are $2P$ mode and closed ones are flaglike modes. The Strouhal numbers of the two modes are well separated, and the Strouhal numbers of $2P$ modes are close to 0.2 whereas those of flaglike modes are above 0.25.

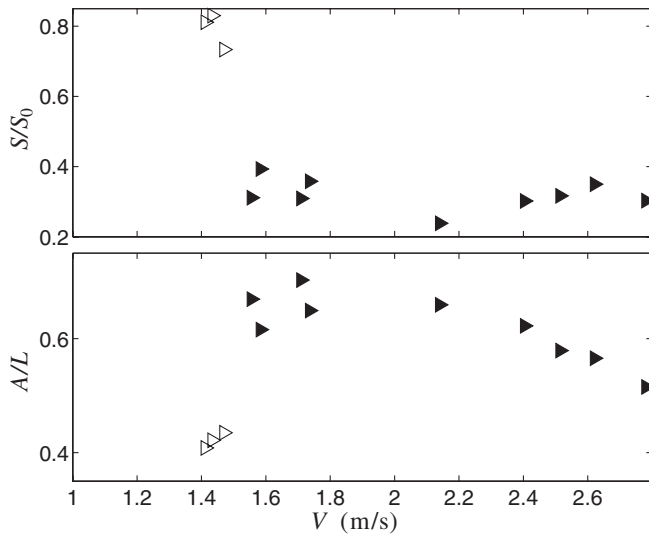


FIG. 5. Enclosed area (upper figure; normalized by $L^2/4\pi$) and amplitude (lower figure; normalized by L) of the oscillating loop for 6 cm loop. Area and amplitude abruptly change as the wake structure transits from $2P$ modes (open symbols) to flaglike modes (closed symbols). As the velocity increases further, the amplitude decreases due to the large drag force.

for $2P$ modes and for flaglike modes are shown in Fig. 4. The $2P$ mode yields St_L approximately 0.2 and the flaglike modes yield values above 0.25.

This separation in the respective Strouhal numbers is caused by a discontinuous change of the amplitude A from the $2P$ mode to the flaglike mode. Figure 5 shows the simultaneous transitions of enclosed area (S) and amplitude (A) of the oscillating loop. At high flow velocity, the streamwise extension of the loop increases due to the higher drag, and this presumably causes the observed relative decrease in enclosed area in the flaglike mode. Because of its now higher aspect ratio, the loop's amplitude increases (compare left and right panels in Fig. 4). The causes of this abrupt change in enclosed loop area and oscillation amplitude remain an open question. Following this abrupt change, the frequency of vortex shedding also increases presumably due to the higher aspect ratio. Unlike the $2P$ mode, the oscillation of the loop and vortex shedding are not in phase, and the wake becomes more complicated.

We have reported on the dynamics of a flexible body as it interacts with an impinging high-speed flow. We find that the loop can have coexisting stable states. In the oscillatory state, the loop oscillation frequency is linearly proportional to the flow velocity and inversely proportional to the square root of the loop length. A linear relation between frequency and velocity is also found in the flow-induced oscillations of loosely mounted cylinders [7,8]. Here, this relationship is explained by a simple model based on the lift force of an

inclined airfoil. With small loop lengths and low flow velocity, a $2P$ wake mode (with pairs of shed vortices [8,21]) is observed and has constant Strouhal number ~ 0.2 . At longer loop lengths and higher flow velocity, a flaglike mode appears with higher Strouhal number (≥ 0.25). This separation in Strouhal numbers is a result of abrupt changes in enclosed loop area and oscillation amplitude.

This work is supported by DOE Grant No. DE-FG02-88ER25053.

-
- [1] D.J. Tritton, *Physical Fluid Dynamics* (Van Nostrand, Princeton, 1977), 1st ed.
 - [2] M.V. Dyke, *An Album of Fluid Motion* (Parabolic, Stanford, 1982), 1st ed.
 - [3] C.H.K. Williamson, *Annu. Rev. Fluid Mech.* **28**, 477 (1996).
 - [4] C.H.K. Williamson and R. Govardhan, *Annu. Rev. Fluid Mech.* **36**, 413 (2004).
 - [5] T. Sarpkaya, *J. Fluids Struct.* **19**, 389 (2004).
 - [6] J.C. Liao, D.N. Beal, G.V. Lauder, and M.S. Triantafyllou, *Science* **302**, 1566 (2003).
 - [7] R. Govardhan and C.H.K. Williamson, *J. Fluid Mech.* **420**, 85 (2000).
 - [8] D. Brika and A. Laneville, *J. Fluid Mech.* **250**, 481 (1993).
 - [9] I. Nakamura, *Phys. Fluids* **19**, 5 (1976).
 - [10] D.G. Karamanev and L.N. Nikolov, *AIChE J.* **38**, 1843 (1992).
 - [11] J. Magnaudet and I. Eames, *Annu. Rev. Fluid Mech.* **32**, 659 (2000).
 - [12] P.C. Duineveld, *J. Fluid Mech.* **292**, 325 (1995).
 - [13] J. Zhang, S. Childress, A. Libchaber, and M. Shelley, *Nature (London)* **408**, 835 (2000).
 - [14] M. Shelley, N. Vandenbergh, and J. Zhang, *Phys. Rev. Lett.* **94**, 094302 (2005).
 - [15] Y. Watanabe, S. Suzuki, M. Sugihara, and Y. Sueoka, *J. Fluids Struct.* **16**, 529 (2002).
 - [16] L. Huang, *J. Fluids Struct.* **9**, 127 (1995).
 - [17] S. Taneda, *J. Phys. Soc. Jpn.* **24**, 392 (1955).
 - [18] Y. Couder, J.M. Chomaz, and M. Rabaud, *Physica D (Amsterdam)* **37**, 384 (1989).
 - [19] M.A. Rutgers, X.-L. Wu, and W.B. Daniel, *Rev. Sci. Instrum.* **72**, 3025 (2001).
 - [20] S. Alben, M. Shelley, and J. Zhang, *Nature (London)* **420**, 479 (2002).
 - [21] C.H.K. Williamson and A. Roshko, *J. Fluids Struct.* **2**, 355 (1988).
 - [22] V.K. Horvath, J.R. Cressman, W.I. Goldberg, and X.-L. Wu, *Phys. Rev. E* **61**, R4702 (2000).
 - [23] W.-J. Kim and N.C. Perkins, *J. Fluids Struct.* **16**, 229 (2002).
 - [24] L.D. Landau and E.M. Lifschitz, *Fluid Mechanics, Course of Theoretical Physics* (Pergamon, Oxford, 1987), Vol. 6, 2nd ed.